J Intell Robot Syst (2016) 84:575–599
DOI 10.1007/s10846-015-0301-4

System Design of a Novel Tilt-Roll Rotor Quadrotor UAV

Abdulkerim Fatih Şenkul · Erdinç Altuğ

Received: 15 December 2014 / Accepted: 28 October 2015 / Published online: 23 November 2015

Abstract Quadrotor helicopters are among one of the most interested topics in the robotics field in the last decade. Regularly, a simple quadrotor has four fixed motors, giving the availability of controlling 4 independent inputs for a 6 degrees-of-freedom (DOF) system. In the recent studies, there is a tendency on changing the controlled system from fixed actuators to the ones that can have dynamic rotations around their axes or planes. This approach is progressing nowadays in order to build more robust versions of quadrotors. The design and control system of a tilt-roll rotor quadrotor has been studied and simulated in this paper. Each of the rotor speeds and their particular angle with respect to the earth frame is adaptively controlled using various control algorithms including cascaded PID. Design implementation of the tiltable geometry is also presented as well as the tilting mechanism's electronic and CAD design. The mathematical model of the tiltable geometry is given and compared with the previous designs by the help of simulations held on Matlab. The simulations prove that the proposed design is more robust and stable than the regular quadrotor especially when environmental limitations are taken into account.

Keywords Tilt rotor · QTR · UAV · Flight stability

A. F. Şenkul
System Dynamics and Control Graduate Program, Istanbul Technical University, İstanbul, Turkey
e-mail: fatihsenkul@gmail.com

E. Altuğ (✉)
Department of Mechanical Engineering, Istanbul Technical University, Istanbul, Turkey
e-mail: altuger@itu.edu.tr

1 Introduction and Motivation

Autonomous unmanned aerial vehicles (UAVs) are one of the most interested fields of study in the last years. They have clear benefits on surveillance and military tasks as well as they can be useful when environmental conditions are not suitable for humans to operate. Thus, the more they become adaptable to the environmental conditions, the more they can handle complicated tasks.

Currently, there are various commercial and experimental UAVs of various sizes available, and many more autonomous unmanned VTOL vehicles are being developed at universities, research centers, and by hobbyists [1–4]. Quadrotor helicopter, a type of VTOL unit, is among one of the most interested topics in the robotics field in the last decade. The quadrotor UAV platform has been used for many applications and research studies, as well. The studies in quadrotor UAV modeling and control increased rapidly in recent years [5–16].

Regularly, a simple quadrotor has four fixed motors, giving the availability of controlling 4 independent inputs values for a 6 DOF system. In order to enhance robustness there is a tendency on the studies

to change the controlled system from fixed actuators into more flexible ones (e.g., motors that can rotate about their axes are used other than fixed).

One of the limiting factor that prevents further implementation of the quadrotor system into applications, is the way quadrotor moves. A quadrotor needs to tilt some degrees along the desired direction of motion. Standard quadrotors are under actuated systems that are required to change their body angles towards the coordinates they are cruising to. By doing this, it can have necessary acceleration towards that direction. But if, there is an onboard camera on board the vehicle, tilting has the undesired effect of moving the onboard cameras' direction of view. This becomes an issue for surveillance and other vision based operations. Since detection or tracking an object becomes a difficult problem as the cameras frame is tilting with the vehicle.

In some certain applications, where there is a lack of working area (e.g., the width or height of the location is too close to the quadrotor's tip to tip length including the propellers), it is not desirable to change the body angle of the quadrotor. It may be more advantages to tilt the rotors instead.

In addition, according to the simulation results those are introduced in this paper, tilting body frame has some undesired effects such as poor stabilization, trajectory tracking and not able to hover at a desired frame angle. The stabilization and hovering skills have also direct effects on the performance of onboard camera recordings and visual guided tasks.

In literature, tilting rotors of a quadrotor was mainly used to convert a quadrotor to an aircraft like vehicle. This combines the advantage of a VTOL vehicle with an aircraft. Quad Tilt Rotor (QTR) is one of the most popular variance of quadrotor airframe. QTR

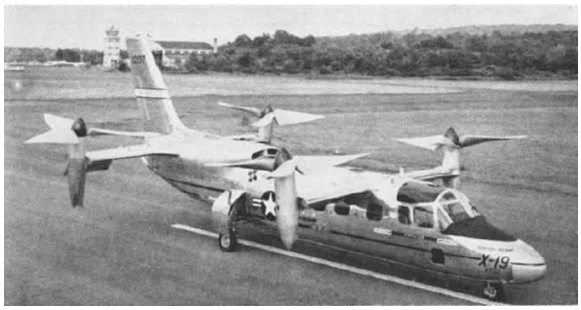

Fig. 1 Curtiss-Wright X-19 Quad-tilt-rotor aircraft developed in 1963

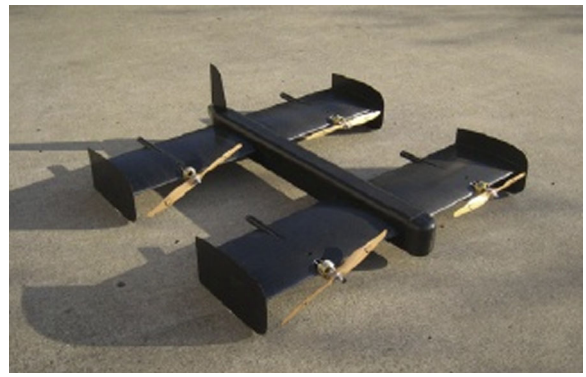

Fig. 2 Tiltable geometry with unmanned quadrotors. Cetinsoy et al. proposed design and construction of a quad tilt-wing UAV

is able to shift between helicopter mode to aircraft mode. This feature enhances the QTR to have extra thrust along the desired axes (front direction) [17, 18].

Curtiss-Wright X-19 QTR aircraft [19] developed in 1963 (Fig. 1), and Bell X-22A [20] was developed 1966 (Fig. 2) are one of the first two prototypes of QTR system on a full-scale.

In literature, another design, named Bell Boeing Quad TiltRotor (V-44) is proposed as a four-rotor derivative of the V-22 Osprey tiltrotor. It is reported to be under development jointly by Bell Helicopter and Boeing [21].

Cetinsoy et al. [22] and Ryll et al. [23] has come up with the idead of tiltable geometry in quadrotors. Quad tilt wing [22] that is illustrated in Fig. 2, is able to tilt their wings in order to adapt itself into either a quadrotor helicopter or a plane. This feature makes the aircraft to vertical take off and land while have relatively better cruising speed with respect to a regular quadrotor. On the other hand Ryll's study

Fig. 3 A quadrotor with regular geometry

[23] is based on a "quadrotor with tilting propellers". Jeong et al. [24, 25] study on omni-directional aircrafts with VTOL and CTOL (Conventional take off and landing) modes are also an enthusiasm for our study on the tilt-roll capable quadrotors. Our previous study [26, 27], was based on a tilt-roll rotor quadrotor that can rotate their rotors in the same direction by tilting and/or rolling movements.

A regular type quadrotor is given in Fig. 3 and illustration of the proposed quadrotor with tilt-roll-able motor geometry is introduced in Fig. 4 for comparison.

The goal of this study is to;

- Design adaptation of a regular quadrotor aiming for better stability and robustness.
- Derive the dynamical model of the proposed vehicle.
- Enhanced maneuver capabilities in constrained environments.
- Change the tilt and roll angles of rotors independently from each other for better adaptability.
- Handle the disturbances more efficiently that occur from nature, environment and hardware imperfections.
- Simulate, compare and improve the quadrotor's performance in terms of robustness, reaching to the destination in lower time, have environment-friendly structure to operate vast numbers of scenarios.

The paper is sorted out as follows: Section 2 portrays the scientific model of the proposed tiltable-rotor quadrotor. The controllers are additionally exhibited to some degree in part B of Section 2. The simulation model and resulting plots that supports the goals of the paper are exhibited in Section 3. Introductory configuration of the tilting instrument and the quadrotor are displayed in Section 4. Closing comments and future work are introduced in Section 5.

Fig. 4 Visualization of the proposed vehicle in this paper

2 Modeling and Control

2.1 Modeling

In this study, the motors are not fixed and are able to tilt-roll separately from each other such that the proposed quadrotor can compensate for unexpected effects that occur from imperfect (real) components or environment. Proposed quadrotor has 12 inputs instead of 4 as in a regular quadrotor due to the additional 2 inputs for each of 4 of the tilting motors. In spite of the fact that these extra control inputs make the framework mechanically more complex, it brings different points of interest by changing over the under-actuated framework to an over-actuated one.

A regular quadrotor is an under actuated helicopter with four rotors that have settled position concerning the vehicle's body frame. In this study, dissimilar to in the general definition, the motors have the capacity to rotate around pitch and roll angles. The obliged energy is created not by tilting body itself, but by tilting the controlled rotors. Table 1 shows the symbols and their definitions that are used through-out the article.

In ideal conditions, it is, by and large, expected that there is no wind penalty on any axes of the quadrotor, all the motors' response time and internal geometries are precisely the same, gyroscopic effects are assumed to be acceptably small and the required thrust vectors that are acquired from the control algorithm can be obtained from the motors without any limitations. Nonetheless, when its all said and done there will be cases in which in specific axes of the multirotor there may exist a constant incorrect output which can be named as bias. Bias may exist by the accompanying reasons: Insufficiencies in actuators, noisy output due to internal and external disturbances, the geometrical flaws of the body frame concerning the perfect framework model, imbalanced propellers and their gyroscopic effects, windy conditions if the flight takes place in outdoor conditions. In this study these negative effects are displayed as one aggravation component called "penalty gain factor".

Table 1 Symbols and definitions

Symbols	Definitions
e_θ	Error of pitch angle
θ_d	Desired pitch angle
θ_a	Actual pitch angle
e_ϕ	Error of roll angle
ϕ_d	Desired roll angle
ϕ_a	Actual roll angle
e_φ	Error of yaw angle
φ_d	Desired yaw angle
φ_a	Actual yaw angle
p	Angular velocity along X axis
q	Angular velocity along Y axis
r	Angular velocity along Z axis
$\dot{p}$	Angular acceleration along X axis
$\dot{q}$	Angular acceleration along Y axis
$\dot{r}$	Angular acceleration along Z axis
β	Initial desired angle value
α	Corrected desired angle value
e_X	Position error along X axis
e_Y	Position error along Y axis
e_Z	Position error along Z axis
$e_{\dot{X}}$	Velocity error along X axis
$e_{\dot{Y}}$	Velocity error along Y axis
$e_{\dot{Z}}$	Velocity error along Z axis
$e_{\ddot{X}}$	Acceleration error along X axis
$e_{\ddot{Y}}$	Acceleration error along Y axis
$e_{\ddot{Z}}$	Acceleration error along Z axis
X_d	Desired position along X axis
Y_d	Desired position along Y axis
Z_d	Desired position along Z axis
X_a	Actual position along X axis
Y_a	Actual position along Y axis
Z_a	Actual position along Z axis
$\dot{X}_d$	Desired velocity along X axis
$\dot{Y}_d$	Desired velocity along Y axis
$\dot{Z}_d$	Desired velocity along Z axis
$\dot{X}_a$	Actual velocity along X axis
$\dot{Y}_a$	Actual velocity along Y axis
$\dot{Z}_a$	Actual velocity along Z axis
$\ddot{X}_d$	Desired acceleration along X axis
$\ddot{Y}_d$	Desired acceleration along Y axis
$\ddot{Z}_d$	Desired acceleration along Z axis
$\ddot{X}_a$	Actual acceleration along X axis
$\ddot{Y}_a$	Actual acceleration along Y axis
$\ddot{Z}_a$	Actual acceleration along Z axis

Table 1 (continued)

Symbols	Definitions
U_T	Throttle Input
F_i	Force Vector
y_θ	Control output for pitch angle
y_ϕ	Control output for roll angle
y_φ	Control output for yaw angle
τ_x	Total torque along x axis
τ_y	Total torque along y axis
τ_z	Total torque along z axis
dT	Sampling Time

Free body diagram of the proposed quadrotor is displayed in Fig. 5. Body fixed frame is thought to be at the focal point of gravity of the quadrotor, where z pivot is indicating downwards concurring N, E, D (North, East, Down) geographical coordinate system. As per the Euler edge representation, edges of revolution about the aircraft's center of mass in x, y and z axes are characterized individually as roll (ϕ), pitch (θ) and yaw (φ) angles respectively. The earth's gravitational force mg is assumed to be constant and in downwards direction with respect to earth frame.

Consider a single motor as demonstrated in Fig. 6. The heading of the thrust vector can be changed by changing the values of pitch (θ_i) and roll (φ_i) angles of the motor where i denotes the motor number i.e. (i: 1,2,3,4). This phenomenon can be represented by a rotation matrix with Euler angles ($\phi_i, \theta_i, \varphi_i$)as in Eq. 1:

$$RPY(\varphi_i, \theta_i, \phi_i) = R(z, \varphi_i) \cdot R(y, \theta_i) \cdot R(x, \phi_i). \quad (1)$$

The resultant force that acts on the quadrotor body frame is denoted by F_i. By using rotation matrix in

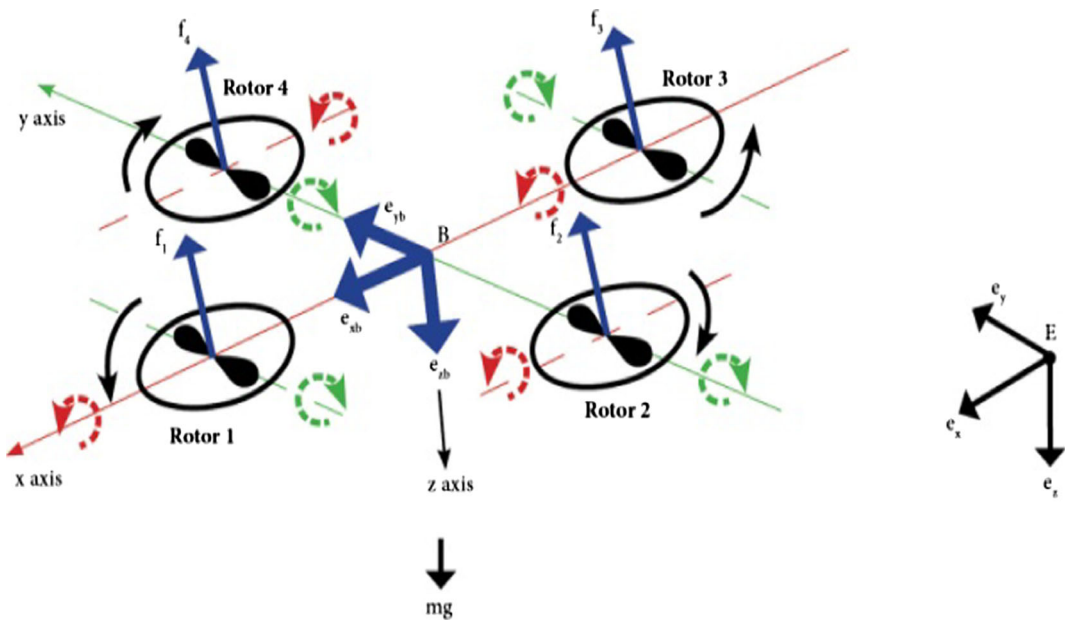

Fig. 5 Free body diagram of Tilt-Roll rotor quadrotor. North-East-Down (NED) geographical coordinate system representation is used

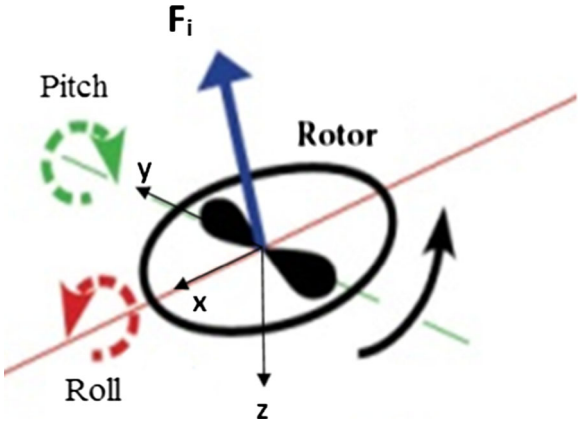

Fig. 6 Rotor angle is changed in order to obtain the required forces in x, y and z directions

Eq. 1 and multiply it with thrust vector for each of the rotors as $F_i \begin{pmatrix} 0 & 0 & -1 \end{pmatrix}^T$ gives the equation in Eq. 2.

$$\vec{F_i} = \begin{bmatrix} F_{ix} \\ F_{iy} \\ F_{iz} \end{bmatrix} = -F_i \begin{bmatrix} Sin(\theta_i) \cdot Cos(\phi_i) \\ -Sin(\phi_i) \\ Cos(\theta_i) \cdot Cos(\phi_i) \end{bmatrix}, \quad (2)$$

$F_{ix}, F_{iy} and F_{iz}$ forces are the components of the thrust force along the x, y, and z axes respectively. Therefore, the resultant force (thrust) vector of each of the rotors can be calculated as follows:

$$F_i = \sqrt{F_{ix}^2 + F_{iy}^2 + F_{iz}^2} \quad (3)$$

The force equation in Eq. 3 is produced by the rotation speeds of the propellers that are denoted as Ω_i, such that Eq. 3 becomes

$$F_i = b{\Omega_i}^2 \quad (4)$$

where b is so-called the push factor.

Tilt and roll angles and their each rotor's rotational speeds can be derived using the formulae in Eq. 5:

$$\begin{aligned} \theta_i &= atan\frac{F_{ix}}{F_{iz}} \\ \phi_i &= asin\frac{F_{iy}}{\sqrt{F_{ix}^2 + F_{iy}^2 + F_{iz}^2}} \\ \Omega_i &= \sqrt{\frac{\sqrt{F_{ix}^2 + F_{iy}^2 + F_{iz}^2}}{b}} \end{aligned} \quad (5)$$

In this study, body angle of the quadrotor with respect to the earth frame is fixed by the user input. In this case we assume that it is zero degrees. In order to achieve this equilibrium the required axial forces to be determined such that the quadrotor will adjust its' motor angles and speed accordingly. Equation 6 gives each of the force values:

$$\sum_{i=1}^{i=4} F_{i_x} = F_x, \sum_{i=1}^{i=4} F_{i_y} = F_y, \sum_{i=1}^{i=4} F_{i_z} = F_z \quad (6)$$

Force vectors on the vertical plane along x direction is necessary to have the hovering motion on our system. In this case, $F_z = mg$ must held in all rotor positions and conditions such that the vehicle can stand still in the z direction by the lead of the altitude control loop. In our case, positive z axis is chosen to be in the opposite direction of the earth's gravity. Therefore, Eq. 7 can be determined as below:

$$\ddot{X}_a = \sum \frac{Fx}{m}, \ddot{Y}_a = \sum \frac{Fy}{m}, \ddot{Z}_a = \sum \frac{Fz}{m} - g \quad (7)$$

Similarly the velocity vectors Eq. 8 can be derived by integrating the acceleration values calculated in Eq. 7.

$$\begin{aligned} \dot{X}_a &= \int_{t=0}^{t=\infty} \left(\sum \frac{Fx}{m} \right) dt, \\ \dot{Y}_a &= \int_{t=0}^{t=\infty} \left(\sum \frac{Fy}{m} \right) dt, \\ \dot{Z}_a &= \int_{t=0}^{t=\infty} \left(\sum \frac{Fz}{m} \right) dt \end{aligned} \quad (8)$$

By having known the moment values in each of the arms, angular accelerations and angular velocities are calculated as in Eqs. 9 and 10 respectively;

$$\dot{p} = \sum \frac{\tau_x}{I_{xx}}, \dot{q} = \sum \frac{\tau_y}{I_{yy}}, \dot{r} = \sum \frac{\tau_z}{I_{zz}} \quad (9)$$

$$p = \int \dot{p}\, dt, q = \int \dot{q}\, dt, r = \int \dot{r}\, dt \quad (10)$$

In Eq. 11 below, M_t denotes the total moments on arms of the quadrotor in which M_d denotes external disturbances, M_{gyro} stands for gyroscopic effects and M_{th} denotes the torque value created along the opposite direction of the rotation of the propeller.

$$M_t = M_d + M_{gyro} + M_{th} \quad (11)$$

Total penalty factor due to disturbances is supposed to be composed of both of $M_d + M_{gyro}$ such that Eq. 11 becomes as in Eq. 12:

$$M_{random} = M_d + M_{gyro} \tag{12}$$

Therefore by linking the parameters in Eqs. 11 and 12 we have;

$$M_t = M_{random} + M_{th} \tag{13}$$

It is expected that M_{random} value is a time-variant random parameter effecting along one axis of an actuator. It represents the unexpected or unpredicted external (i.e. wind gusts) and internal (i.e. propeller imbalance, imperfections of the body frame or instabilities-transient responses of electrical motors) disturbances.

For the sake of computation and simulation, x vector is chosen as the effected axis (it is up to the user to choose whether it is x, y or z axes) when modeling.

We introduce a penalty gain factor, f_{pe} to the system. f_{pe} represents the total disturbance factor (including gyroscopic effects) on the actuator (i.e. electric motor and the propeller in this case). We let this gain to be time-variant and spontaneously take values from 0.1 to 1.9. In fact this parameter can be equal to any polynomial which equals to the following: $1.9 > f_{pe}(t) > 0$. in any given time t. In this case force gains of F_{x_i} and F_{z_i} of the quadrotor is directly related with $F_{pe}(t)$. The model and the control system is based on keeping attitude and altitude control of the vehicle while changing the propeller speeds and motor angles of each actuator.

In Fig. 7, the free body diagram proposed model is given, where β is the desired angle and α is the corrected angle value which depends on $F_{t_{new}}$. The diagram shows the force vectors of F_x, F_z, F_t, $F_{t_{new}}$ on x-z plane of the quadrotor.

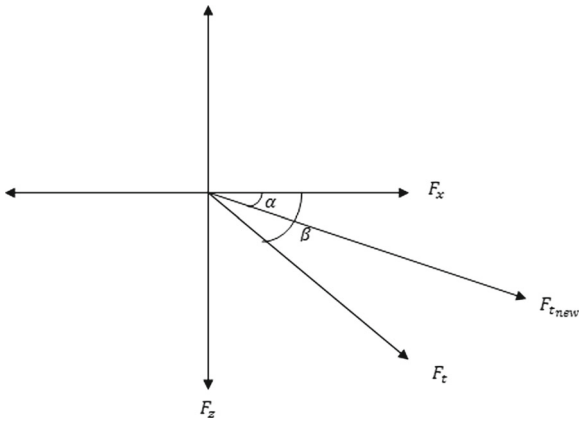

Fig. 7 Free body diagram of a motor that is adaptively corrected with new angle and force values

2.2 Control

The control of the tilt-roll rotor quadrotor differs from the regular quadrotor. In this section, proposed controllers are presented. In this work, the control algorithm is designed such that all the motors tilt with same angle values depending on the control output. This approach simplified the control work significantly, at a cost of reducing the potential benefits of the vehicle.

Calculating the $\dot{\theta}_i$ and $\dot{\phi}_i$ value of a single motor would be sufficient in terms of controllability of the system. This concept of this study lets all of the four motors to rotate at the same speed so that they produce the same amount of resultant forces $F_1 = F_2 = F_3 = F_4$. This will be different, if the motors act separately from each other with different rotational speeds and rotational angles. This concept will be considered in the future work.

For performance and applicability purposes, cascaded PID control is chosen for control and simulation of the proposed aircraft. There exists total of 4 cascaded PID loops where each of motor angles are controlled with the inputs received from the vehicle's position, velocity, altitude and total force vectors (Fig. 7). In order to control all of these inputs, the following equations should be satisfied:

$$\begin{aligned} F_{i_x} &= \frac{y_\theta}{4}, F_{i_y} = \frac{y_\phi}{4} \\ F_{1_z} &= F_{3_z} = \frac{U_T}{4} + \frac{y_\varphi}{4} \\ F_{2_z} &= F_{4_z} = \frac{U_T}{4} - \frac{y_\varphi}{4} \end{aligned} \tag{14}$$

where throttle, U_t, is applied as an input in order to increase/decrease motor speeds so that the aircraft can increase, decrease or maintain its altitude (hover position).

For control purposes the angle errors must be determined. The pitch angle error is calculated using the formula in Eq. 15.

$$e_\theta = \theta_d - \theta_a \tag{15}$$

Then control output, y_θ is determined using the following PID loop:

$$y_\theta = Kp * e_\theta - Kd * p + Ki * \frac{d}{dt} \sum_{t=0}^{t=\infty} E_{\theta(t)} \quad (16)$$

The corresponding equations for (ϕ) and (φ) control outputs can be written as Eqs. 15, 16 by changing the (θ) terms by (ϕ), (ω) and $(\dot{\theta})$ terms by $(\dot{\phi})$, $(\dot{\varphi})$.

For velocity and position control of the aircraft following equations are used:

$$e_X = X_d - X_a \quad (17)$$

$$\dot{X}_d = \frac{Kp * e_X}{dT} - Kd * \dot{X}_a \quad (18)$$

$$e_{\dot{X}} = \dot{X}_d - \dot{X}_a \quad (19)$$

$$\theta_d = Kp * e_{\dot{X}} - \frac{Kd * \ddot{X}_a}{dT} \quad (20)$$

Similarly, roll angle (ϕ) estimation of motors with respect to position and velocity output can be calculated using equations (17)–(20) by replacing (X), $(\dot{X})$, $(\ddot{X})$, (θ) with (Y), $(\dot{Y})$, $(\ddot{Y})$, (ϕ), respectively.

For altitude hold control of the aircraft, equations in Eq. 21 are used:

$$e_Z = Z_d - Z_a$$
$$U_T(t) = U_t(t-1) + Kp * e_Z - Kd * \frac{(\dot{Z})_a}{dT} \quad (21)$$

By controlling current throttle parameter in Eq. 21, one can control the altitude of the vehicle. It is useful to control the throttle value by using a feedback loop for a robust design for altitude hold purposes.

Note that the control output values in PID loops are constrained in safe limits so that the aircraft would not make too aggressive maneuvers.

In this study the adaptive control of the aircraft is designed assuming that the aircraft will go towards to one direction at a time in 2D space. In the examples and formulation given in modeling and control chapters these axes are chosen to be X and Z. An adaptive control algorithm for tilt-roll rotor quadrotor is proposed. In order to stabilize the system in Fig. 8 the following expressions must be calculated:

$$F_z = F_t * \sin(\beta) \quad (22)$$
$$F_{x_{gained}} = F_t * \cos(\beta) * f_{pe} \quad (23)$$

where $F_{x_{gained}}$ represents the final value of F_x if no adaptive stabilization is applied on this axis (i.e. less than desired x force, F_x if $f_{pe} < 1$ and more if vice versa). Thus, if $f_{pe} = 1$ then $F_{x_{gained}} = F_x$

Similarly;

$$F_x = F_t * \cos(\beta) \quad (24)$$

After adding the new angles and force vectors we get:

$$F_x = F_{t_{new}} * \cos(\alpha) * f_{pe} = F_t * \cos(\beta) \quad (25)$$
$$F_z = F_{t_{new}} * \sin(\alpha) = F_t * \sin(\beta) \quad (26)$$

New resultant force can be estimated as in the following:

$$F_{t_{new}} = F_t * \frac{\cos(\beta)}{\cos(\alpha) * f_{pe}} = F_t * \frac{\sin(\beta)}{\sin(\alpha)} \quad (27)$$

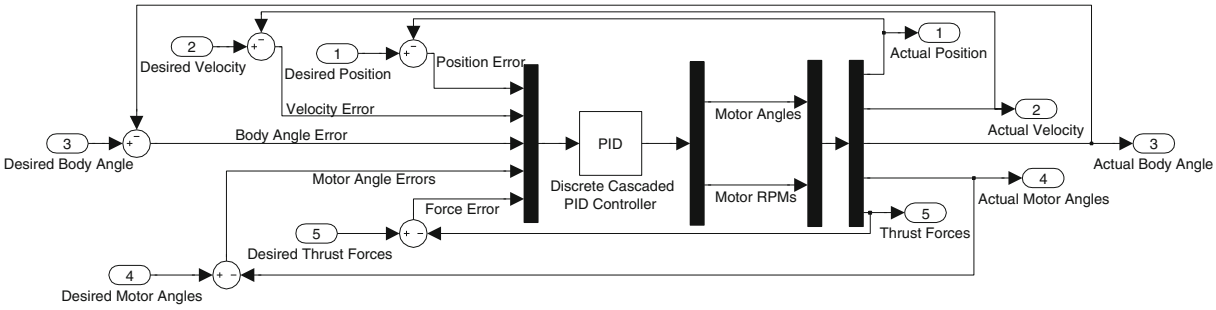

Fig. 8 Simplified cascaded block diagram of tilt-roll rotor quadrotor

This is equal to the following equalities;

$$\begin{aligned} F_{t_{new}} * \cos(\alpha) * f_{pe} * \sin(\alpha) &= F_t * \cos(\beta) * \sin(\alpha) \\ &= F_t * \sin(\beta) * \cos(\alpha) * f_{pe} \end{aligned} \tag{28}$$

By using Eq. 28, the adapted angle, α is obtained as follows:

$$\alpha = \tan^{-1}\left(f_{pe} * \tan\beta\right) \tag{29}$$

In Fig. 8 a simplified block diagram of the control algorithm of a tilt-roll rotor quadrotor is given. In adaptive version, the motor angles and speeds are controlled according to the above formulation with an extra feedback closed loop system.

For instance, the initial desired angle value, β is calculated from the cascaded PID algorithm. The outputs are rotation speeds of the propellers, required force vectors along axes and angle values of the motors and the vehicle (nominal value is zero degree) where thrust vector total is denoted by F_t. Further calculations are done as f_{pe} is introduced to the control system as shown in Eq. 23. As an example, penalty gain factor can be a constant that equals to 0.9 on z axis such that actual Z force would be equal to 0.9 times the desired value of the control output. Thus, it is not likely for the quadrotor to balance itself with the existence of such force and torque vector inequalities. Therefore, resultant force F_{t_i} is updated according to the adapted force vector of $F_{t_{new_i}}$ that's introduced in Eqs. 27 and 28.

Adaptive control tilt-roll rotor is determined by the fact that there is a proportional relation between desired angle and adapted angle (β-α) versus the change in the speeds of the rotors, Ω_i such that if (β-α) gets smaller and Ω_i is expected to decrease and when (β-α) gets larger Ω_i is expected to increase. If (β-α) = 0 this indicates that Ω_i will not change at all.

3 Simulations

In this section, the simulation results and the performance of the proposed control systems will be introduced.The designed models and control systems are simulated in Matlab-Simulink for verification and comparison. Dynamical behaviors of the regular, non-adaptive tilt roll and adaptive tilt roll quadrotors will be introduced. In this part, the cons and pros of each system will be overlayed after each simulation.

During the simulations, the vehicle's angle against earth is held at zero degrees by the controllers. However, it can be held upto ±30 degrees in both of roll (ϕ) and/or pitch (θ) angles for tilt-roll rotor and adaptive tilt-roll rotor versions. But for regular quadrotors it is not possible to fix the roll and pitch angles to a user pre-defined value. Therefore, for simplicity in understanding and comparing the various control systems, we choose zero degree angle as the target fix angle (hover position for regular quadrotors). Nevertheless, yaw angle φ of all of the quadrotors can be changed during the simulations.

The initial values of roll, pitch and yaw angles (ϕ, θ and φ) can be defined at the beginning of the simulation. What's more, the start point and target destination points can also be initialized in terms of x, y and z axes. If needed (only in non-auto flight mode in manual control) throttle value of the quads can be trimmed and modified during the flight simulation.

First simulations are held between regular versus non-adaptive tilt roll quadrotors (Figs. 9, 10, 11, 12, 13 and 14). In order to compare in the same conditions we set the starting and target finish points the same. Initial and cruise inputs are set as in the following: The starting point is set as x=1, y=1, z=0 and target finish point is set at x=18, y=18, z=8 on Matlab coordinate system. In the starting position the quads have -10 degrees of yaw angle, φ. Then at t=1, vehicles are requested to change their heading from -10 to +10 degrees and at t=6, to 0 (zero) degrees. In addition to this, the quads are set to zero degree of roll (ϕ), pitch (θ) angles at the start point.

3.1 Yaw Performance Comparison

In the first simulation tilt-roll rotor quadrotor's dynamic performance of yaw control is observed (Fig. 9). As seen in the graph, the settling time to get to the desired angle is quite small (about 0.2 seconds at most) without any overshoot.

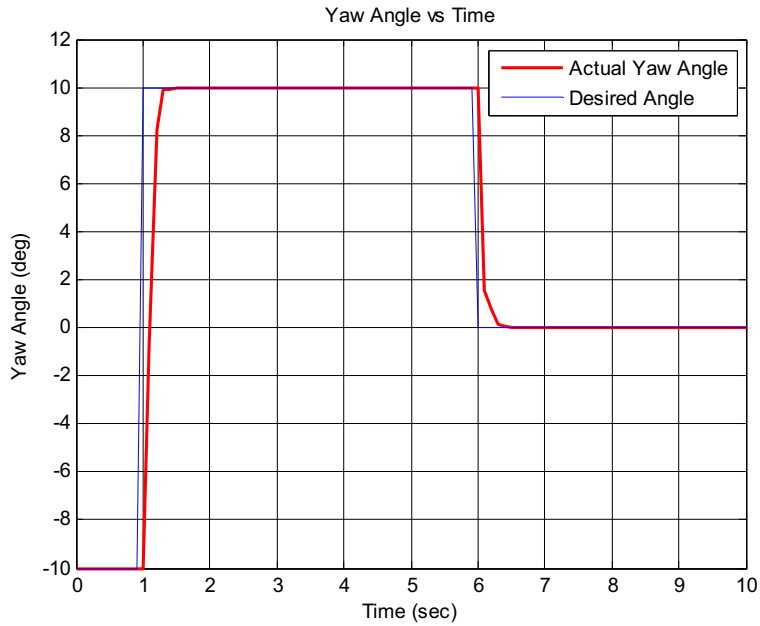

Fig. 9 Tilt-roll rotor quadrotor yaw angle (φ) vs time simulation

3.2 Regular vs Tilt-Roll Rotor Quadrotor

Regular quadrotor and non-adaptive tilt-roll rotor quadrotor are plotted in Figs. 10, 11 and 12 as they fly from the predefined starting point to the desired 3D coordinate of x=18, y=18, z=8.

Results show that tilt-roll quad has relatively have lesser settling time in the attitude control performance compared to a regular quadrotor. In the altitude control, although regular quad is leading to reach the desired z coordinate, it has more overshoot with respect non-adaptive tilt-roll quad. This kind of

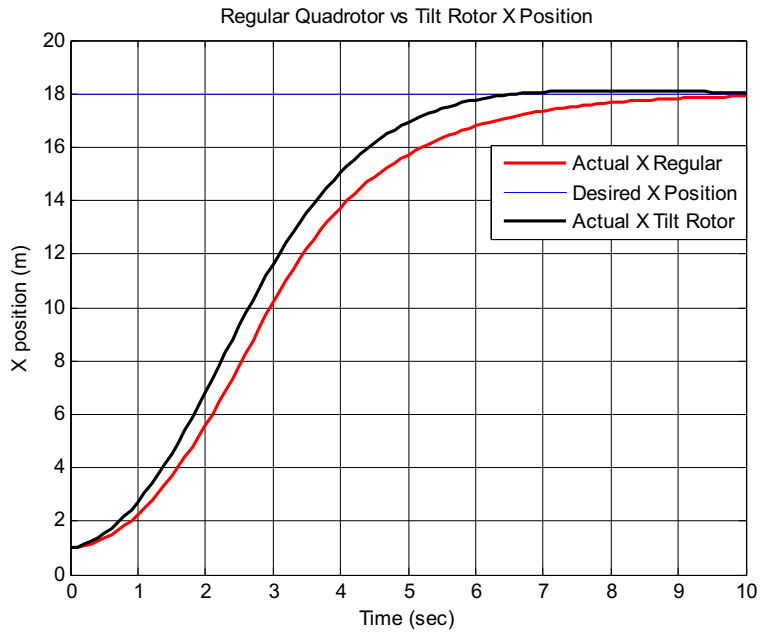

Fig. 10 Regular vs. Tilt-roll rotor settling to desired position (x)

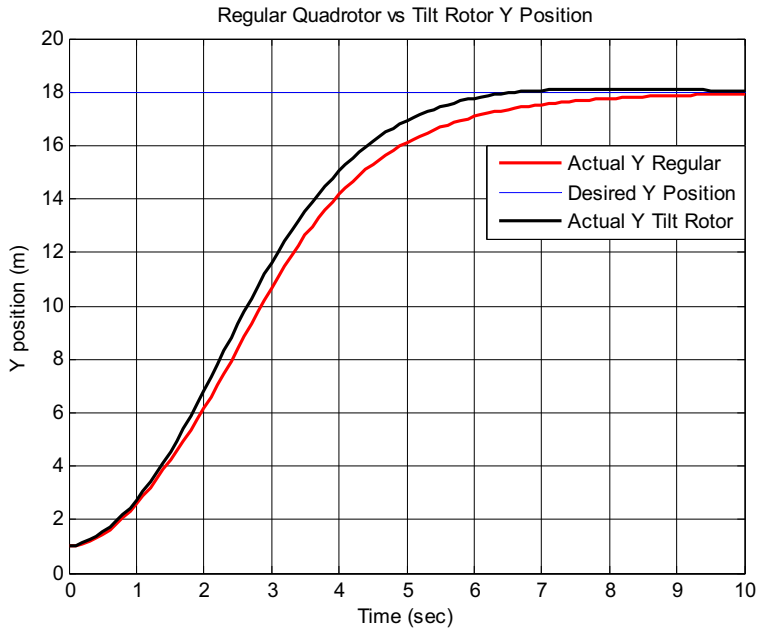

Fig. 11 Regular vs. Tilt-roll rotor settling to desired position (y)

dynamical behavior may not be desired in some certain situations where stabilization takes important role such as photo-shooting.

After all, both of the quads are controlled with intricate 13 diverse PID parameters. That is the reason extra tuning is possible by changing these coefficients so that both of the quads' performances may change.

The greatest advantage acquired by the tilt-roll rotor quadrotor is because of how it moves. It moves by tilting the rotors, rather than tilting the airframe

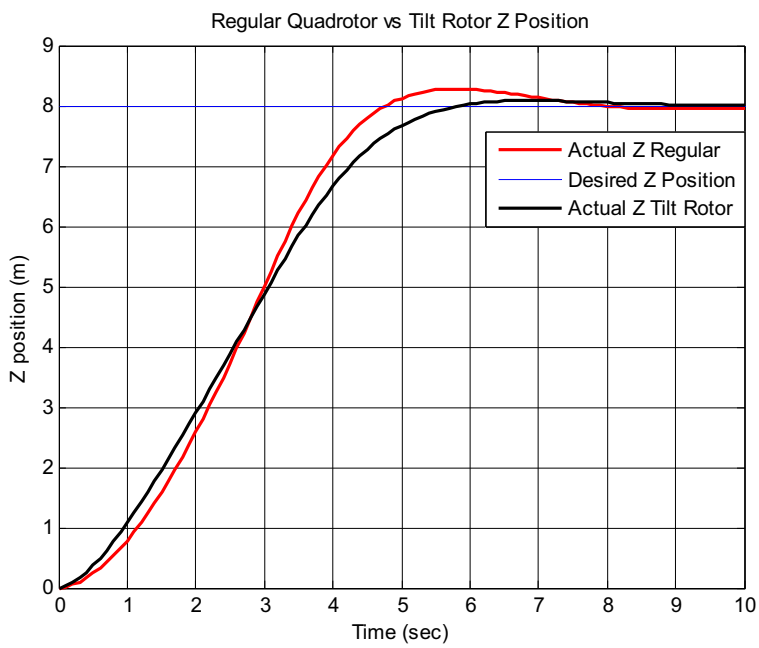

Fig. 12 Regular vs. Tilt-roll rotor settling to desired position (z)

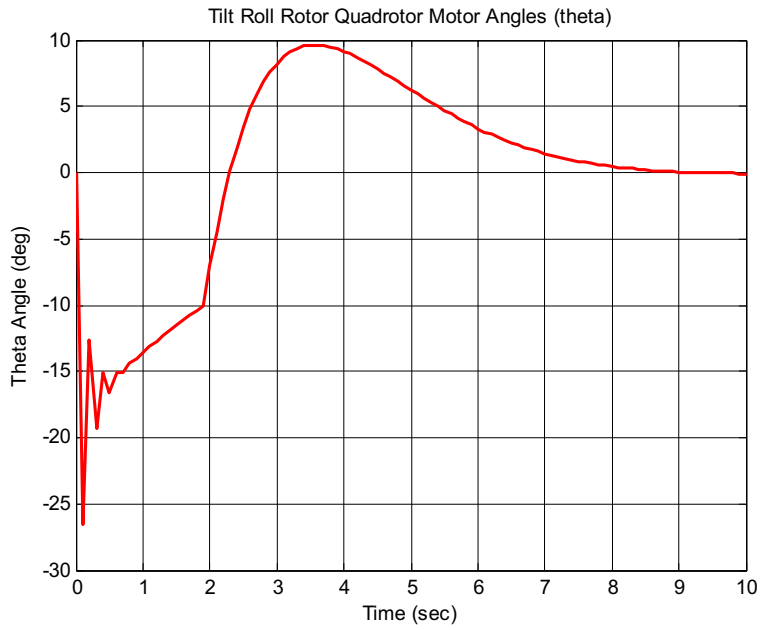

Fig. 13 Tilt-Roll Rotor quadrotor's motor angles (theta)

as the standard quadrotors do. The capacity of tilting rotors guarantees a more steady flight of the airframe. The tilt (theta) and roll (phi) of rotors during the previous simulation is plotted on Figs. 13 and 14. The starting angles of pitch (θ) and roll (ϕ) are zero and equal to each other. That's why both of the plots of theta and phi angles precisely match one another on these graphs.

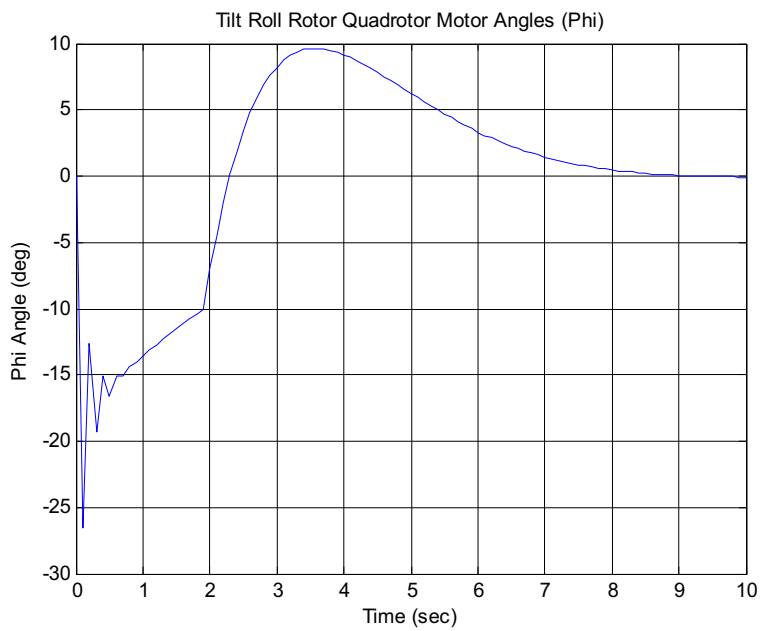

Fig. 14 Tilt-Roll Rotor quadrotor's motor angles (phi)

3.3 Comparison of Regular, Tilt-Roll Rotor and Adaptive Tilt –Roll Rotor Quadrotors

The third simulation is designed such that all of the regular, non-adaptive and adaptive quadrotors' dynamical performances can be compared. The same trajectory is followed by all of the 3 quadrotors along x and z axes. Quad1, is a regular quadrotor with fixed rotors, Quad2, is non-adaptive tilt-roll rotor quadrotor [26], Quad3 is the adaptive tilt-roll rotor quadrotor. It is capable of tilting their rotors as Quad2 does. In addition to this it can adaptively modify each of its rotors such that it can adapt itself to random changes due to environment and/or internal defects of actuators or propellers. Quad3 is able change its rotor speeds and angles independently from each other [27] while Quad2 is only capable of changing all the rotor angles at the same time in the same direction.

In the third simulation all of the three quadrotors are observed with a penalty gain, f_{pe} of 1. Hence, there is no effect of the penalty gain against quadrotors' flight abilities. The results can be seen in the Figs. 15 and 16.

Figures 15 and 16 show the comparison of flight performances between a regular quadrotor versus tilt roll rotor quadrotors with different control algorithms (i.e. Quad2 has non-adaptive control algorithm while Quad3 has adaptive). The results prove that Quad2 and 3 have better settling time values than Quad1. Moreover, maximum overshoot value of Quad1 is larger (worse) than the other two quads. On one hand, the fact that Quad2 and Quad3 have better stabilization than Quad1 is not suprising as we have already investigated the performance characteristics and show that tilt-roll rotor quads perform better than regular quads in Figs. 11 and 12 [26]. On the other hand, we see that the tracjectory curves of Quad2 and Quad3 are almost matching with each other. This is due to the fact that the penalty gain, f_{pe} is equal to 1 – no negative effect on systems. Therefore, we can not clearly see the advantage of the adaptive control of Quad3 over Quad2 in this example. That's why we have

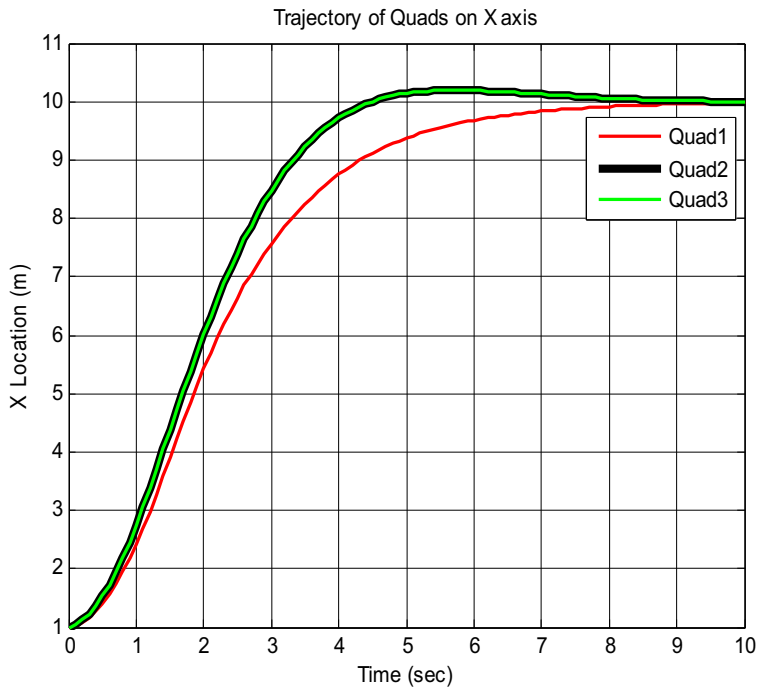

Fig. 15 Simulation results with a penalty gain of 1 on X axis

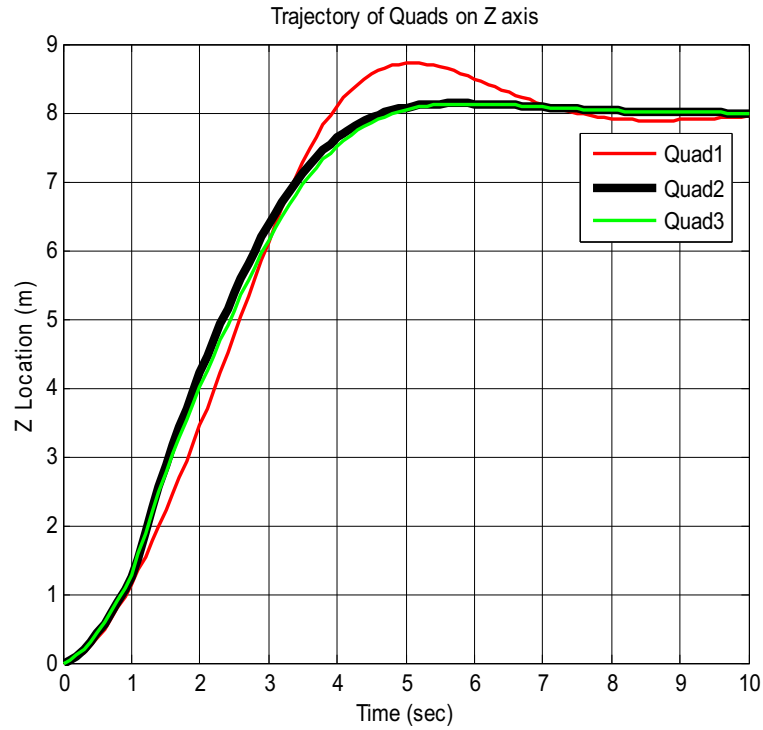

Fig. 16 Simulation results with a penalty gain of 1 on Z axis

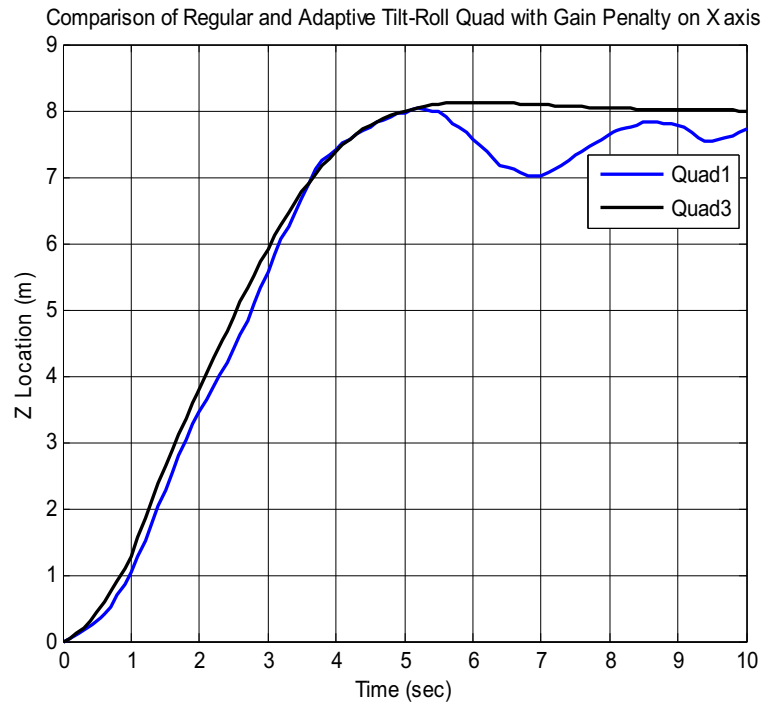

Fig. 17 Fourth simulation result: Penalty gain randomly changes between 0.1 and 1.9 on Z axis for both of the quads

simulated fourth and fifth simulations as in the following sub-chapters.

3.4 Regular vs Adaptive Tilt – Roll Rotor Quadrotors with Random Penalty Gains on 1 Axis

The fourth simulation is carried out in order to observe the effects of penalty gain, f_{pe} on quadrotors' stabilization and trajectory tracking features. In this example, f_{pe} is a random variable that spontaneously takes values between 0.1 to 1.9. The rest of the simulation initial settings are set as before as in the third simulation.

Normally this simulation was designed to take part for all of the three types of quadrotors. Unfortunately, Quad2 has lost all of its' track during the simulation and go beyond the graph in Figs. 17 & 18. Hence, we have plotted only Quad1 and Quad3 for this simulation. After doing several further investigation on the results, we've managed to find the critical tolerance values of f_{pe} in which Quad1 is somewhat on the track. Then f_{pe} is set to be equal to 0.95 as a constant value through-out the fourth simulation. Please note that Quad2 can not survive even with this penalty gain factor. Therefore, it can not be observed within this simulation.

In Fig. 17 the comparison of the regular quadrotor versus adaptive controlled quadrotor is plotted with a random penalty gain effectin on both of the systems. In the first 5 seconds Quad1 is able to track the path. Trajectory curves of Quad1 and Quad3 are very similar to each other within this time interval of t=0 to t=5. However, after t=5, Quad1 losses its track and begins to oscillate such that it never ever keep up the track and locate itself to the target reference point. On the other hand, Quad3 gets to the reference point smoothly, without any oscillations, over-shoots and undesired coordination changes during its flight. In fact the performance characteristics of Quad3 is more or less the same with the third simulation. This shows that Quad3 is able adapt itself to negative and undesired effects of the random penalty gain.

3.5 Not Adaptive vs Adaptive Tilt – Roll Rotor Quadrotors with Fixed Penalty Gains on 1 Axis

In order to compare Quad2 and Quad3, one more simulation is run such that penalty gain is fixed to a constant value of 0.95. Please see Fig. 18 for the plotted graph.

Although penalty gain is constant and relatively smaller than in simulation presented in Section 3.4,

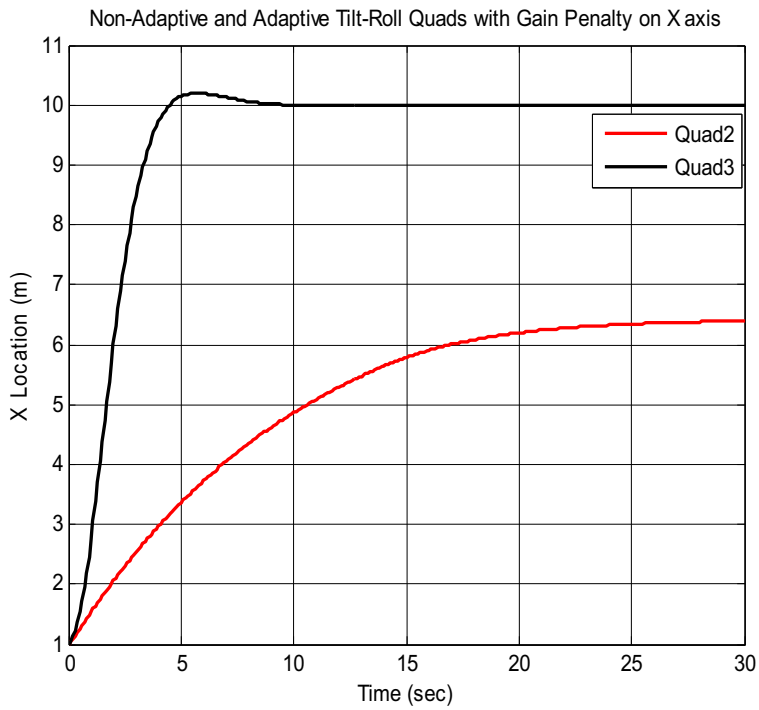

Fig. 18 Fourth simulation result: Penalty gain of non-adaptive tilt roll is fixed to 0.95. Penalty gain randomly changes between 0.1 and 1.9 for adaptively controlled quad

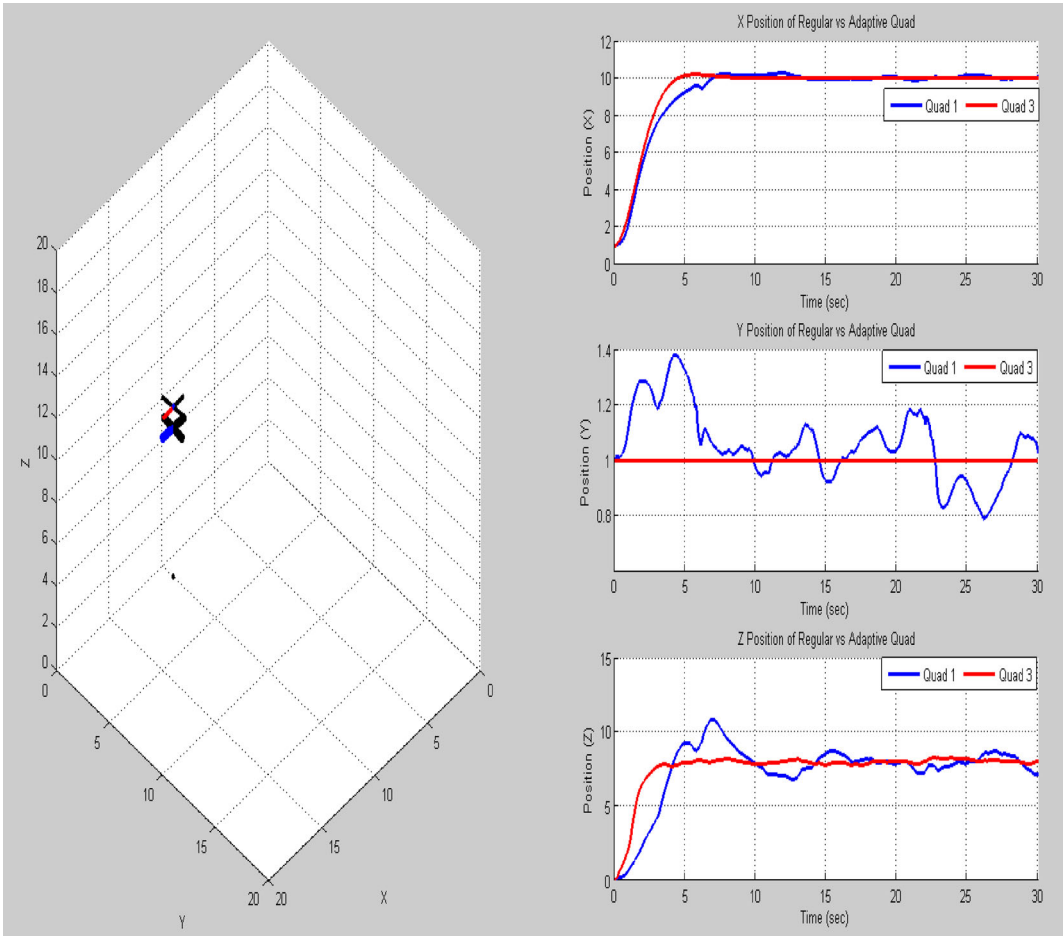

Fig. 19 Penalty gain (F_{pe}) is applied to all of the axes of the quadrotors. (F_{pe}) is randomly changing from 0.3 to 1.7 for each of the axes, x, y and z

Quad2 has failed to reach to the desired x coordinate of 10. Instead, as seen on the graph Quad2 tends to settle to about 6.5 point in about 30 seconds of time interval. On the other hand, Quad3 can get to exactly the desired position of x=10 in about 10 seconds. Quad3 can estimate the constant error on the actuators and adaptively correct its' propeller angles and speeds in order to reach the desired coordinates.

3.6 Regular vs Adaptive Tilt – Roll Rotor Quadrotors with Random Penalty Gains on all Axes

Lastly, two more simulations have been run in order to compare the flight performance characteristics of the regular quad vs. adaptive controlled tilt-roll rotor quad. Unlike in the previous simulations, this time penalty gain, F_{pe} is applied to all of the axes of quadrotors other than only one. In order to have apple-to-apple comparison with the previous simulations, at first arbitrary changing F_{pe} values are fixed between 0.3 to 1.7 as demonstrated in Figs. 19 and 20. In Fig. 19, 3D coordinates plot and 3 subplots are added. Subplots show the x, y and z axes outputs of the regular quad (Quad 1) and adaptive tilt-roll rotor quad (Quad 3). The snapshot is taken in the last second of the simulation at t=30.

As seen on 3D coordinates plot of Fig. 19, Quad 1, represented with blue heading line, seems unable to reach desired position of (10,1,8) coordinates unlike Quad 3 which is represented with red heading line. By deep-diving into sub-plots, it is clear that Quad 1 has a oscilatory response when settling to the X

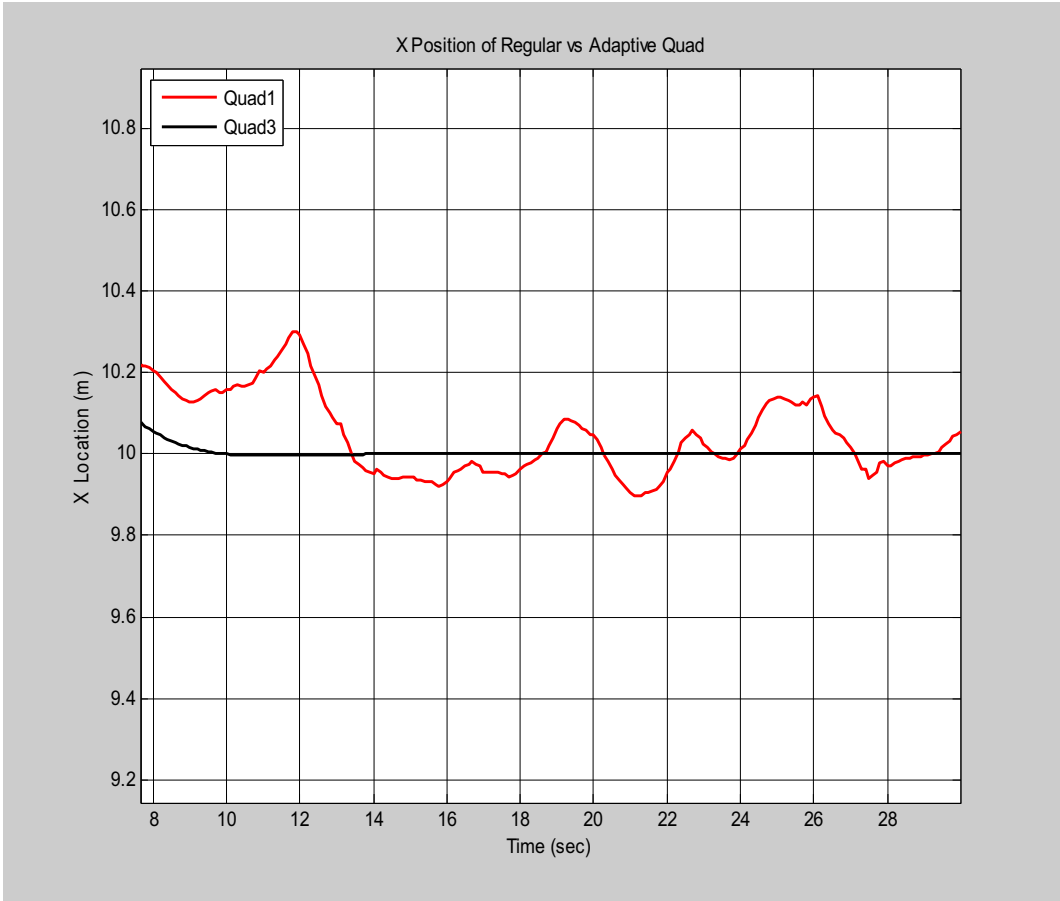

Fig. 20 Zoomed in version X axis trajectories of two quads on Fig. 19

axis coordinates (Please see focused plot at X axis response of each of the quadrotors in Fig. 20). In this figure, the Quad 1 has an oscilation around 9.8 to 10.3 points.

On Y axis response on the second subplot of Fig. 19, although the trajectory is defined from (1, 1, 0) to (10,1,8) coordinates without any change in Y axis, Quad 1 is can be said to be negatively affected by the random penalty values resulting with unexpected sudden changes during its cruise. As seen on the second subplot there are some rough coordinate changes although it does not need to change its Y axis track from the beginning. Unlike Quad 1, Quad 3 holds its track solid and still on Y axis by keeping Y axis value of 1. In z axis response on the third subplot, it is noticable that Quad1 is unable to track its path smoothly and at the end of 30 seconds it reaches a value lower than the target z axis value of 8 on Matlab coordinates frame. This result can also clearly be seen from the 3D coordinates plot on the west side of Fig. 19. However, Quad 3 proves that it has achieved to overcome each of the axes' penalty gains and settles to the desired coordinates of (10,1,8) at the end.

In the following simulation, penalty gain (F_{pe})'s variation is decreased such that it can take arbitrary values from 0.8 to 1.2. It is again applied to all of the axes of Quad 1 and Quad 3 as in the previous simulation.

According to the graphs plotted in Fig. 21, it can be seen on 3D Figure that the performance of the Quad 1 increased with the decreased variation of the penalty gain. That's why both of Quad 1 and Quad 3 seem to overlap each other on their final position on 3D graph. This also proves that the irregular behavior of the regular quadrotor is directly related with the variations of F_{pe}. On the other hand, Quad 3's cruise characteris-

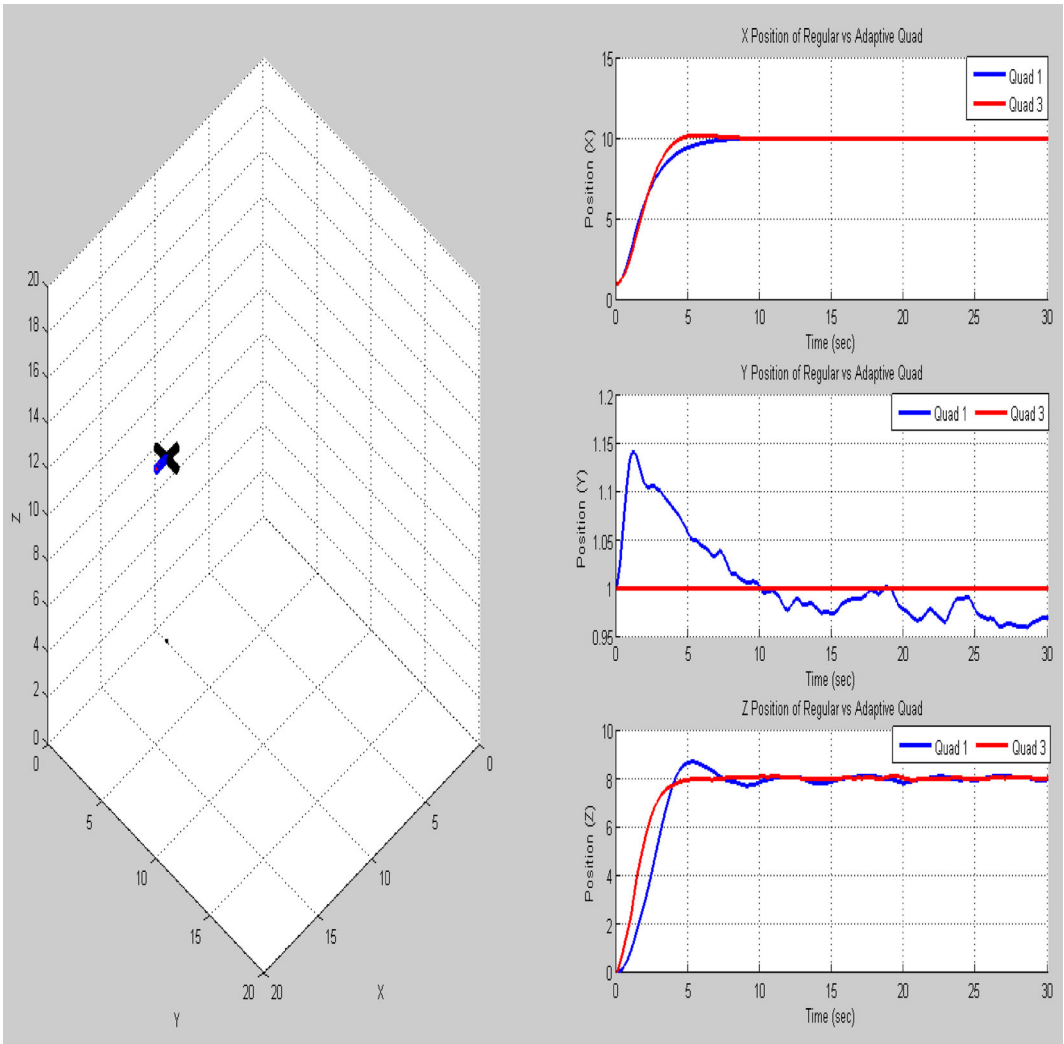

Fig. 21 Penalty gain (F_{pe}) is applied to all of the axes of the quadrotors. F_{pe} is randomly changing from 0.8 to 1.2 for each of the axes, x, y and z

tics are more or less the same as it can keep up with dynamically varied values of disturbances. Only it can be noted that with the lesser variation of F_{pe}, Quad 3 has less oscillatory behavior. Please see Fig. 22 for more focused version of Z axis nearby the settling point of 8.

4 System Design

In this section, mechanical and electrical design of the proposed quadrotor will be introduced. The following topics are covered: The designed and modeled frame specifications, dimensional features of the propellers and their characteristics, introduction to the tilting mechanism, actuators used in the mechanical system, tilting mechanism's electrical configuration and the specifications of the actuators used.

The proposed systems block diagram is shown in Fig. 23. Beside the mechanical frame and tilting mechanism, a control computer resides at its core. 12 electronic speed controllers (ESC), control the 12 motors to give desired motion.

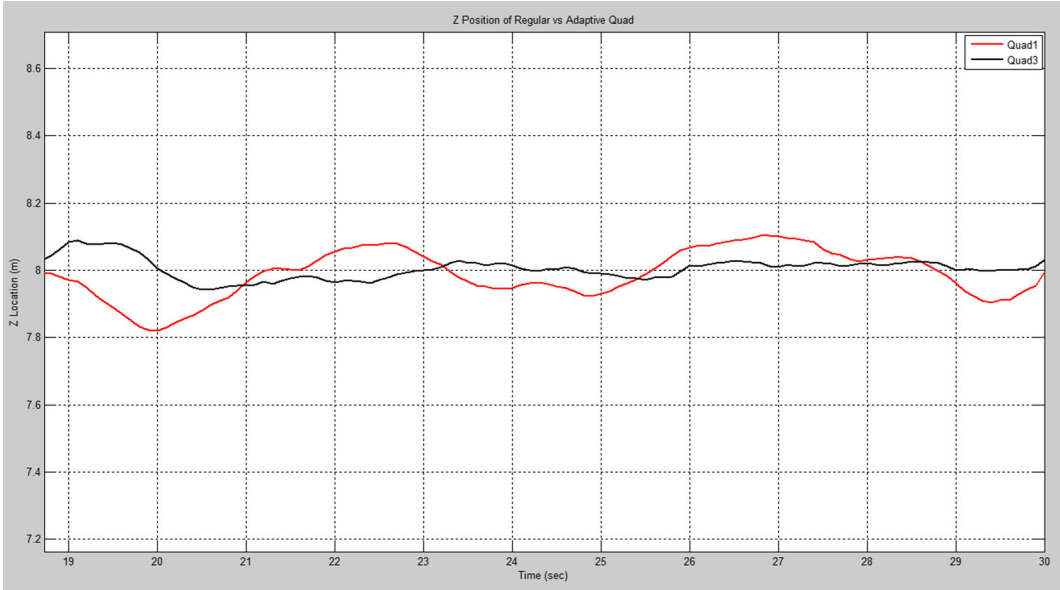

Fig. 22 Zoomed in version of Fig 21 around the settling point on Z axis

4.1 Main Design

There are mainly two frames considered in this paper. One of them is built in our ITU lab to simulate the results and connections of the sub-systems. The other frame is considered to be Wookong's flamewheel as we have already tested its' performance in another Quadrotor project. The specs of the frame, flamewheel is as in the following [28]:

- Frame Weight:478g
- Diagonal Wheelbase:550mm

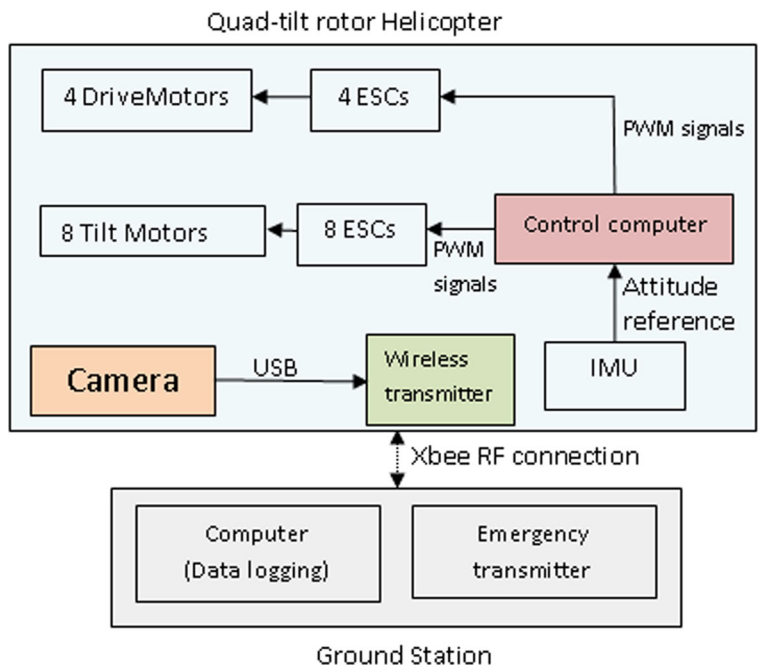

Fig. 23 Block diagram of the proposed system

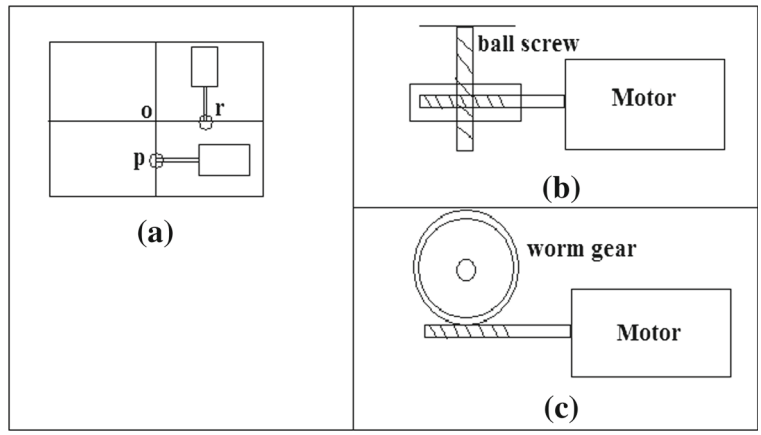

Fig. 24 Proposed tilting mechanism

- Takeoff Weight:1200g ˜2400g
- Recommended Propeller:10 ×3.8in ; 8 ×4.5in
- Recommended Battery:3S˜4S LiPo
- Recommended Motor:22 ×12mm (Stator size)
- Recommended ESC:30A OPTO

Recommendations specified above are taken into consideration when determining the take-off weight, sizes of propellers, capacities and voltage range of batteries, stator sizes of electrical brushless motors and ESCs.

Choosing the appropriate brushless motors for the quadrotor system is crucial as they are directly related with the thrust force generated and delivered to the system. What's more, by the use of the propellers, the total drag force is generated. This drag force is related with propellers' pitch angle and K_V value (motor velocity constant) of the brushless rotors. Therefore, as the drag force gets higher, the usage of battery power increases. In the proposed quadrotor, the most important feature for the actuators is to provide high thrust force due to the fact that estimated mass of the

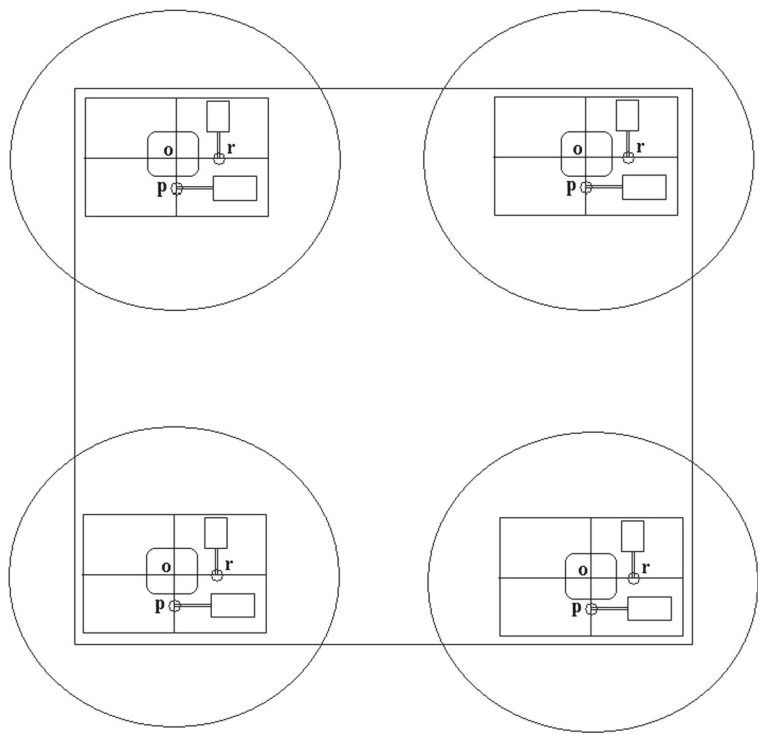

Fig. 25 Initial design of proposed quadrotor

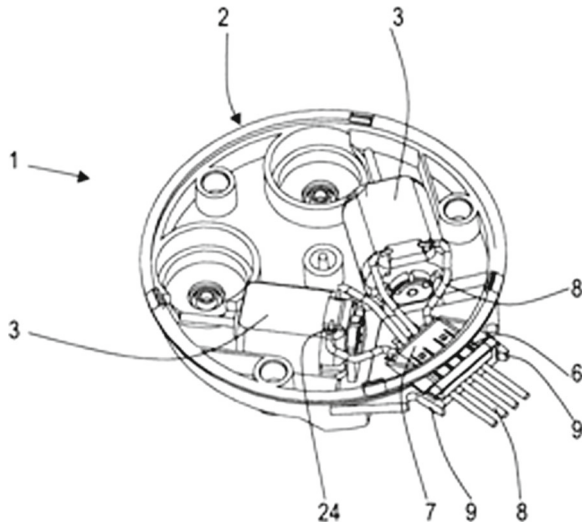

Fig. 26 A car mirror tilting mechanism [29]

quadrotor is 2.2kg including the tilting mechanism. In addition to this, propellers are constrained to tilt up to 15 degrees such that this feature requires the rotors to rotate faster in order to hold the quadrotor in altitude control as described in the control section of this paper.

According to the facts given above, high performance brushless T-motors [31] were chosen as main actuators. These brushless electrical motors have K_v values of 900 and give thrust values as high as 1kg per each arm if used with 10 x 4.5 inches diameter propellers which we will use on our system.

Propellers for the quadrotor are chosen such that the necessary thrust forces can be obtained even if the propellers are in tilted position due to the proposed control algorithm. Therefore, we first choose the adequate brushless motors which will be introduced in the actuators section, and their pairing propellers. For this reason, $900K_v$ brushless electrical motors are paired with Ideafly's 10x4.5 inches carbon propellers.

4.2 Tilting Mechanism Design

The proposed quadrotor requires four tilting mechanisms. The mechanisms should be low weight, are able to hold the resistance torques, and enable the pitch and roll motions independent of each other.

One possible solution to the design came from patent search of tilting mechanisms. Authors [29] proposed a similar mechanism for tilting car mirrors.

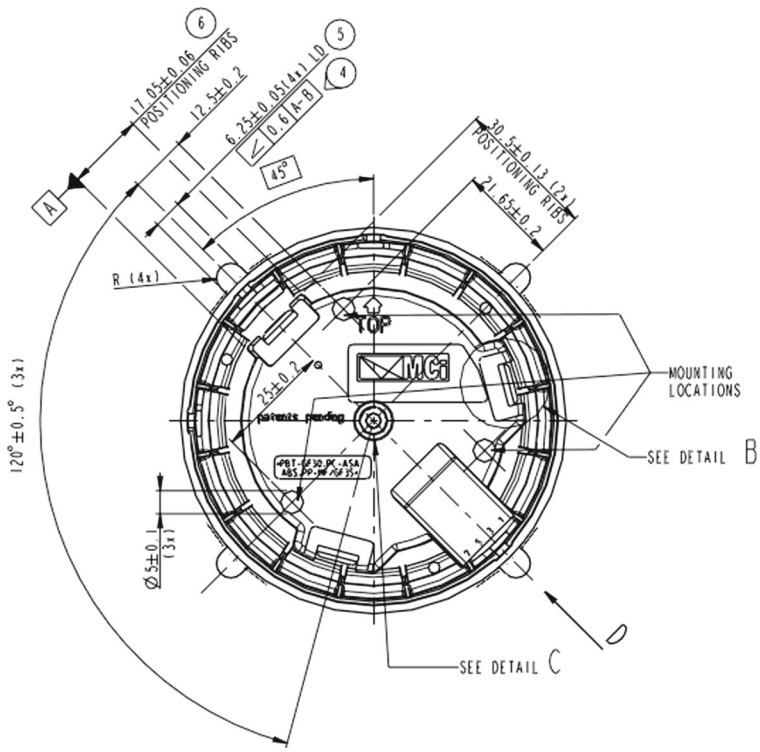

Fig. 27 2D drawing of an automatic wing mirror actuator (*Top* view)

Table 2 General product specifications of MCI wing mirror actuators [30]

Description	Specification
Actuator dimensions	Top level drawing 3XXXXX{**SC**}
Actuator color	Black
Application mirrorglass weight up to*	0.365 [kg]
Working temperature range (Tb)	$-40 < Tb < 85$[°C]
Working voltage range (Ub)	$9 < Ub < 16$[VDC]
Supply voltage potentiometer (Um)	$4.7 < Um < 5.3$[VDC]

In order for the proposed system to function properly, the tilting mechanism examples are examined from the similar systems. The control system itself sets the limitations of ±15 degrees of tilt and roll motion for each of the rotors. Therefore, an off-the-shelf tilting mechanism that is able to provide these angle values both in pitch and roll directions with a robust control would be sufficient. After some research, within these specs in the bag, the relatively easier and robust way to turn a regular quadrotor into a tilt-roll rotor quadrotor is achieved by using automatic car wing mirror actuators. They are easy to use, can be run by using simple electronics tools within a proven robustness level. Not only these but also they already have both of tilt and roll control system in the box once their operational plane lay-out is rotated 90 degrees along x axis.

A simple lay out of the wing mirror is given in Fig. 24.

Figure 24a shows the top view of the tilting platform. Lift generating motor and rotor sets will be placed on each platform. The points P and R, are

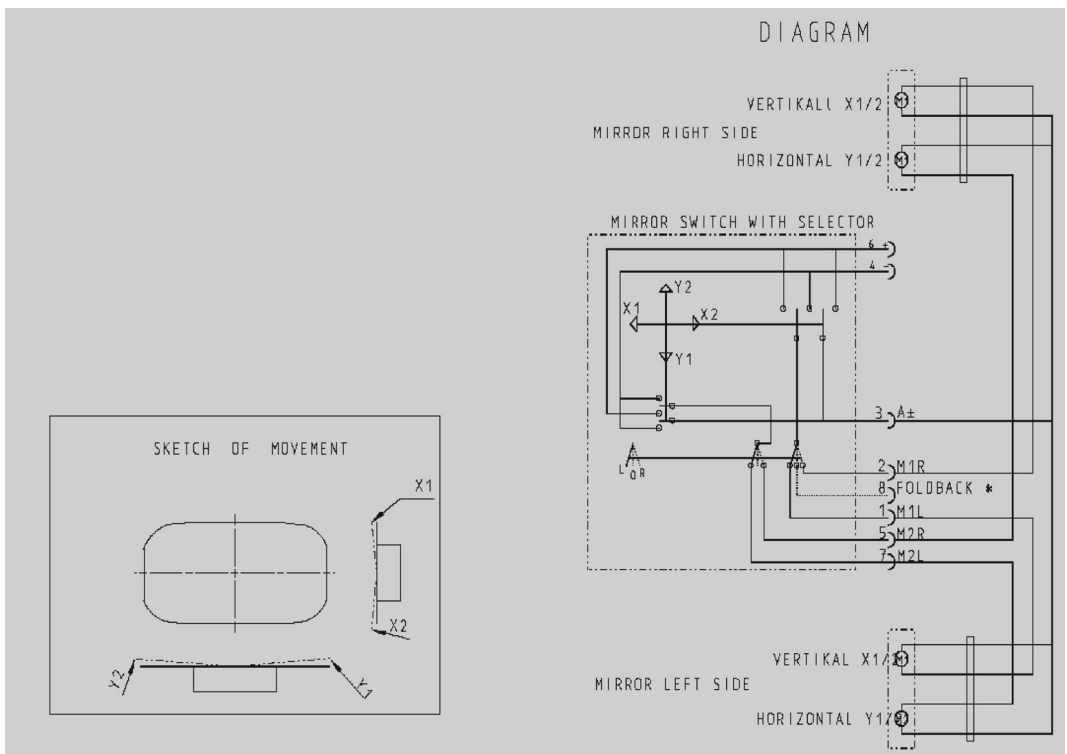

Fig. 28 2D circuit diagram for tilting mechanism

Table 3 Functional measurement data of MCI wing mirror actuators

Description	Specification
Actuator weight (m)	< 0.135[kg]
Travel angle (S)	$2.6 \pm 2[^\circ]$
Freeplay (St)	$< 0.4[^\circ]$
Traveling speed (ω)	$3 < \omega < 4.5[^\circ/s]$**{SC}**

where the platform is actuated to have pitch and roll motions, respectively. The mechanism will tilt with respect to the center point O.

Each motor shaft has a worm which attached to a worm gear as shown in the top view in Fig. 24c. This arrangement reduced rotational speed and allows higher torques to be transmitted to the tilting mechanism. The worm gear has a ball screw inside as shown in side view of Fig. 24b, which will rise and lower the platform as required.

The height of the ball screw mechanism and the distance between points O, R and P determine the pitch and roll limits of the mechanism. Please see Figs. 25 and 26 for the 2 DC motor driven schematics of wing mirror actuator design.

Figure 25 shows the proposed quadrotor with the tilting mechanisms are mounted. Figure 26 shows inner view of one of these tilting mechanisms. Each mechanism requires two micro DC motors for tilt and roll motions.

In this project, the tilting mechanism of the proposed tilt-roll rotor quadrotor is based on Mirror Controls International (MCI) wing mirror actuators. These wing mirrors are used on some Ford vehicles. The 2D drawings of the actuator system and the specifications obtained from the datasheet of the wing mirror actuation system are given in Fig. 27 and Tables 2 and 3.

As this actuator system will be driven to hold the quadrotor in desired positions according to the feedback control loop explained in the control section of this paper, the product specifications and limits should be understood well. The following tables of MCI actuators' general product and functional measurement data are requested from the supplier.

The actuator system can be driven between the voltage intervals from 9V to 16V as given in Table 2. Therefore, it was decided to use one 3S Lithium polymer (LiPo) battery to drive both of the electronic board, tilting mechanism (i.e. MCI wing mirror actuators) and the electrical brushless motors.

As seen on Table 3, one of the actuator's weight is 135 grams. Since the tilting of four rotors will require 4 of these mechanisms, a total of 540 grams of additional payload are introduced. This amount can be compensated by the use of high efficiency brushless motors and propellers as described previously. The travelling speed (ω) is also sufficient enough for the quadrotor to respond to minor change of motions within 3 to 4.5 degrees per second.

Electrical circuit design of the tilting mechanism is introduced in Fig. 28. The rotation of the axes and horizontal-vertical control inputs are given according to this diagram. In the tilt-roll system on the quadrotor, X1 and X2 are used for tilt motion of the rotors and Y1 and Y2 are used for roll motion of the rotors. The ground connection is fixed the same with the main Li-Po batteries and control board of the quadrotor.

4.3 Conceptual Design of Tilt-Roll Rotor Quadrotor

In the automation systems laboratory, a representative conceptual design of tilt-roll rotor quadrotor was built with prototype level parts. Please see Fig. 29 for the initial photo of the quadrotor.

In this design, MCI's car wing mirror tilting mechanism is successfully transferred to the quadrotor system. By using this tilting mechanism, it is

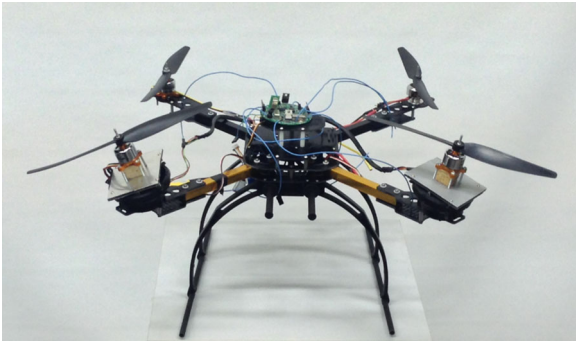

Fig. 29 Conceptual design of tilt-roll rotor quadrotor with prototype parts

possible to change four of the rotors surface planes along x and y axes with tilt and roll motions. In the Figure it is already clear that the front motors (#1 and #4) are both tilted and rolled different angles with respect to the quadrotor frame of reference.

5 Conclusions and Futureworks

In this paper control, modeling and system design of a novel quadrotor that can tilt and/or roll its rotors is introduced. Simulations are presented in order to compare the performances of the tilt-roll rotor quadrotor with respect to the regular – standard quadrotors in terms of their reliability and robustness. Moreover, tilt-roll rotor quadrotor has also been compared with the same layout with different control algorithms. Those algorithms are consisting of either cascaded PID or cascaded PID with adaptive correction to random disturbances. Having compared these, adaptively corrected tilt-roll rotor quadrotor's performance is found to be relatively better than the other versions. Therefore, preliminary system design has been done in our lab for doing tests to verify the simulation outcomes.

In real life, there are so many unknown or complex parameters that cannot be calculated and modeled before the flight of an aircraft. What's more, it is always a possibility that the actuators of the aircraft can be lacking of performance such that the desired output delivered is out of tolerances. The main focus of this paper is to develop a quadrotor that can overcome undesired disturbances whose sources can be any dynamical system components of the vehicle or the environment. It is made clear in the simulations that by using adaptively corrected tilt-roll rotor, it is possible to eliminate or at least compensate the errors due to those disturbances. With this study, ordinary fixed rotors are switched into tilt-able ones. The proposed quadrotor can adaptively update its rotor angles and their speeds to compensate for undesired conditions.

As opposed to the standard version, tilt-roll rotor quadrotors have further benefits other than the robustness and reliability during flight. Tilt-roll rotor quadrotors are capable of hovering at user input body angles and this feature enables them to pass through narrow paths that may be shorter in width of the quadrotor. This enchances the multicopter to have flexibility advantage in rugged conditions of uses where working spaces have rather complex fixed geometries or geometries that dynamically change (i.e. in case of fire condition inside a house). Furthermore, this feature leads the tilt-roll rotor quadrotors to dodge obstacles and unknown attacks without changing or manipulating its attitude or altitude control.

In the future works of this project, once all of the design-intend parts are received as explained through system design section of this paper, tilt-roll rotor quadrotor will be re-built such that the tilting arms can be controlled firstly, from a remote controller manually and then, automatically according to the control inputs obtained.

Acknowledgments This work was supported in part by the Scientific and Technological Research Council of Turkey (TÜBİTAK) under Grant 114M765.

References

1. Castillo, P., Lozano, R., Dzul, A.E.: Modelling and Control of Mini-flying Machines, Advances in Industrial Control series, ISSN 1430-9491 (Springer)
2. Chao, H.Y., Cao, Y.C., Chen, Y.Q.: Autopilots for small unmanned aerial vehicles: a survey. Int. J. Control. Autom. Syst. **8**(1), 36–44 (2010)
3. Lee, D., Kaminer, I., Dobrokhodov, V., Jones, K.: Autonomous feature following for visual surveillance using a small unmanned aerial vehicle with gimbaled camera system. Int. J. Control. Autom. Syst. **8**(5), 957–966 (2010)
4. Han, D., Kim, J., Min, C., Jo, S., Kim, J., Lee, D.: Development of unmanned aerial vehicle (UAV) system with way point tracking and vision-based reconnaissance. Int. J. Control. Autom. Syst. **8**(5), 1091–1099 (2010)
5. Hamel, T., Mahony, R., Lozano, R., Ostrowski, J.: Dynamic modeling and configuration stabilization for an X4-flyer. In: Proceedings of IFAC 15th Triennial World Congress, Barcelona (2002)
6. Altuğ, E., Ostrowski, J.P., Taylor, C.J.: Control of a quadrotor helicopter using dual camera visual feedback. Int. J. Robot. Res. **24**(5), 329–341 (2005)
7. Suter, D., Hamel, T., Mahony, R.: Visual servo control using homography estimation for the stabilization of an X4-flyer. In: Proceedings of the 41st IEEE Conference on Decision and Control, pp. 2872–2877 (2002)
8. Moktari, A., Benallegue, A.: Dynamic feedback controller of Euler angles and wind parameters estimation for a quadrotor unmanned aerial vehicle. In: Proceedings of the IEEE Conference on Rob. and Auto., pp. 2359–2366 (2004)
9. Dunfied, J., Tarbouchi, M., Labonte, G.: Neural network based control of a four rotor helicopter. In: Proceedings of IEEE International Conference on Industrial Technology, pp. 1543–1548 (2004)

10. Earl, M.G., D'Andrea, R.: Real-time attitude estimation techniques applied to a four rotor helicopter. In: Proceedings of IEEE Conference on Decision and Control, pp. 3956–3961 (2004)
11. Slazar-Cruz, S., Palomino, A., Lozano, R.: Trajectory tracking for a four rotor mini-aircraft. In: Proceedings of the 44th IEEE Conference on Decision and Control and the European Control Conference, pp. 2505–2510 (2005)
12. Escareno, J., Salazar-Cruz, S., Lozano, R.: Embedded control of a four-rotor UAV. In: Proceedings of the American Control Conference, pp. 189–204 (2006)
13. Bouabdallah, S., Siegwart, R.: Backstepping and sliding-mode techniques applied to an indoor micro quadrotor. In: Proceedings of the IEEE Conference on Robotics and Automation, pp. 2247–2252 (2005)
14. Beji, L., Abichou, A., Zemalache, K.M.: Smooth control of an X4 bidirectional rotors flying robot. In: 5th International Workshop on Robot Motion and Control, pp. 181–186 (2005)
15. Castillo, P., Dzul, A.E., Lozano, R.: Real-time stabilization and tracking of a four-rotor mini rotorcraft. IEEE Trans. Control Syst. Technol. **12**(4), 510–516 (2004)
16. Tayebi, A., McGilvray, S.: Attitude stabilization of a VTOL quadrotor aircraft. IEEE Trans. Control Syst. Technol. **14**(3), 562–571 (2006)
17. Gaffey, T.: Large cargo rotorcraft bell helicopter's perspectives. AHS Forum, 56 (2000)
18. Yeo, H., Johnson, W.: Performance and design investigation of heavy lift tilt-rotor with aerodynamic interference effects. J. Aircr. **46**(4), 1231–1239 (2009)
19. Borst, H.V.: Design and development considerations of the X-19 VTOL aircraft. Ann. N. Y. Acad. Sci. **107**, 1749–6632 (1963)
20. Hirschberg, M.J.: An Overview of the History of Vertical and/or Short Take-Off and Landing (V/STOL) Aircraft. In: Proceedings www.vstol.org (2006)
21. Sklar, M.: Diversity in design. Boeing Frontiers Magazine, pp. 44–45, December 2006–January 2007 issue (2006)
22. Cetinsoy, E., Dikyar, S., Hancer, C., Oner, K.T., Sirimoglu, E., Unel, M., Aksit, M.F.: Design and construction of a novel quad tilt-wing UAV. Mechatronics **22**, 723–745 (2012)
23. Ryll, M., Bülthoff, H.H., Giordano, P.R.: Modeling and Control of a Quadrotor UAV with Tilting Propellers. 2012 IEEE International Conference on Robotics and Automation River Centre. Saint Paul, pp. 4606–4613 (2012)
24. Jeong, S.H., Jung, S.: Novel Design and Position Control of an Omni-directional Flying Automobile (Omni-Flymobile). In: International Conference on Control, Automation and Systems 2010, pp. 2480–2484. KINTEX, Gyeonggi-do (2010)
25. Salazar-Cruz, S., Lozano, R., Escaren, J.: Stabilization and nonlinear control for a novel trirotor mini-aircraft. Control. Eng. Pract. **17**, 886–894 (2009)
26. Şenkul, F., Altuğ, E.: Modeling and Control of a Novel Tilt – Roll Rotor Quadrotor UAV. In: Proceedings of IEEE International Conference on Unmanned Aircraft Systems (ICUAS'13) Atlanta, pp. 1071–1076 (2013)
27. Şenkul, F., Altuğ, E.: Adaptive Control of a Tilt – Roll Rotor Quadrotor UAV. In: Proceedings of IEEE International Conference on Unmanned Aircraft Systems (ICUAS'14), pp. 1132–1137, Florida (2014)
28. Wiki. Dji: Flame Wheel F550 Specifications", retrieved, December 06, 2014 from http://wiki.dji.com/en/index.php/Flame_Wheel_F550_Specifications (2013)
29. Guttenberger, R.: Actuating mechanism for driving a motor vehicle rearview mirror. patent number: US6419368 B1, http://www.google.com/patents/US6419368
30. MCI: Product specification. Mirror actuator 300 series, Code: SPE0099, Rev:7 (2010)
31. T-Motor: Safest propulsion system. retrieved December 10, 2014 from http://rctigermotor.com/ (2014)

Abdulkerim Fatih Şenkul received the B.S. degree in mechatronics engineering from Sabancı University in 2010, the M.S. degree in System Dynamics and Control engineering from Istanbul Technical University in 2015.

His work career has started at Atlantis Unmanned Vehicle Solutions company as a Mechatronics and Control Engineer in 2011. He has worked on Control system design of an autonomous quadrotor, Aeroseeker, and an autonomous unmanned underwater vehicle, Aquaseeker for 2 years. He has started working as a Powertrain Program Management & Integration Engineer under Product Development branch of Ford Motor Company in 2012. During his 3 years of experience he has worked mainly on Ford Cargo Trucks. He is currently working as a consultant engineer at Altran in Belgium.

His research interests are mainly on design and control of unmanned aerial vehicles, and intelligent systems design.

Erdinç Altuğ received the B.S. degree in mechanical engineering from Middle East Technical University in Ankara, in 1996, the M.S. degree in mechanical engineering from Carnegie Mellon University in 1999, and the Ph.D. degree in mechanical engineering from the University of Pennsylvania in 2003.

He joined in Istanbul Technical University in 2004, where he is currently an Associate Professor in the Department of Mechanical Engineering. His research interests are vision-based control of robotic systems, stabilization and control of unmanned aircraft systems, industrial automation & control, and mechatronics.